

Daily concentration of snowfalls in the mountains of the Iberian Peninsula

Marc Lemus-Canovas^{1,2} | Esteban Alonso-González³ | Josep Bonsoms⁴ |
Juan I. López-Moreno⁵ 

¹Andorra Research + Innovation, Sant Julià De Lòria, Andorra

²CRETUS Institute, Nonlinear Physics Group, Department of Particle Physics, Faculty of Physics, Universidade de Santiago de Compostela, Galicia, Spain

³Centre d'Etudes Spatiales de la Biosphère (CESBIO), Université de Toulouse, CNES/CNRS/IRD/UPS, Toulouse, France

⁴Department of Geography, Universitat de Barcelona, Barcelona, Spain

⁵Instituto Pirenaico de Ecología (IPE-CSIC), Zaragoza, Spain

Correspondence

Marc Lemus-Canovas, Andorra Research + Innovation, Sant Julià De Lòria, Andorra.

Email: mlemus@ari.ad

Funding information

Spanish Ministry of Science and Innovation, Grant/Award Number: PID2021-124220OB-100; Xunta de Galicia (Government of Galicia, Spain), Grant/Award Number: ED481B-2022-055; Spanish Ministry of Science, Innovation and Universities, Grant/Award Number: PRE2021-097046

Abstract

The temporal concentration of snowfalls has direct implications on the management of water resources as well as on the economic activity of mountain areas, conditioning, for example, the seasonal performance of ski resorts. This work uses the daily concentration index (CI) for analysing the frequency concentration of snowfalls in the Iberian Peninsula Mountain ranges. First, we provide a spatiotemporal analysis of the CI patterns and trends for the 1980–2014 period. Subsequently, we determine the atmospheric circulation patterns that control the CI variability. In addition, we determine the geographical and low-frequency climate modes that control the CI for this mid-latitude area. In addition, we have estimated the partial dependence relationship between the CI and several geographical factors by fitting a multiple linear regression. The results from these analyses show that elevation as well as the distance from the Atlantic are the main geographical pattern that controls the CI in the Iberian Peninsula Mountain ranges. These geographical factors also reflect the role of the main atmospheric circulation patterns in the Iberian Peninsula in controlling the spatial dynamics of the CI. The Cantabrian, Iberian, and northern slopes of the Pyrenees show the lowest CI due to their exposition to northern and Atlantic circulation weather types. On the contrary, the highest CI values are found in the southern and eastern slopes of the Pyrenees, eastern slopes of Sierra Nevada, and southern slopes of the Central system. Trend analysis shows a slight increase of CI in the Central system and in the western Sierra Nevada. However, eastern Sierra Nevada, Cantabrian, Central, and Iberian show a downward CI trend. CI is principally driven by the East-Atlantic/Western Russia pattern and the North Atlantic Oscillation (NAO) in the Cantabrian, Iberian, and northern slopes of the Central range. The CI values in the Pyrenees show a different relationship with the Western Mediterranean Oscillation (WeMO) depending on whether it is the southern or the northern slope. In addition, the positive phase of the NAO oscillation controls the higher values of CI for the whole Pyrenees, especially in the

This is an open access article under the terms of the [Creative Commons Attribution-NonCommercial](https://creativecommons.org/licenses/by-nc/4.0/) License, which permits use, distribution and reproduction in any medium, provided the original work is properly cited and is not used for commercial purposes.

© 2023 The Authors. *International Journal of Climatology* published by John Wiley & Sons Ltd on behalf of Royal Meteorological Society.

mid-south part. Finally, in Sierra Nevada the CI dynamics are controlled mostly by the WeMO.

KEYWORDS

concentration index, Iberian Peninsula, low-frequency climate modes, snowfall, synoptic patterns

1 | INTRODUCTION

The mountainous snowpack is an important factor in alpine zones, controlling the hydrology and the dynamic of alpine ecosystems (Wipf & Rixen, 2010). It governs the greening onset of alpine vegetation (Chen et al., 2015; Revuelto et al., 2022), geo-ecological dynamics (Kreyling & Henry, 2011), and serve as a thermal insulator, protecting the soil from freezing (Liebezeit et al., 2014) and freeze–thaw cycles (Wang et al., 2020). Additionally, snowpack also influences biochemical processes (Segura et al., 2019) and becomes a crucial freshwater resource for lowland areas (Adam et al., 2009).

Iberian mountain ranges, are key zones for runoff generation (Morán-Tejeda et al., 2014), supplying an important portion of the water used by agricultural, industrial, and touristic sectors (e.g., Lorenzo-Lacruz et al., 2010). As in other Mediterranean regions, Iberian snowpacks are characterized by a high intra- and inter-annual variability (Fayad et al., 2017) due to significant year-to-year precipitation variability (Vicente-Serrano & Trigo, 2011) and a relevant decadal climatic oscillation (Lionello et al., 2014). Winter temperature and precipitation are primarily controlled by atmospheric circulation variability (Lemus-Canovas, 2022; Saffioti et al., 2016) governed by low-frequency climate mode oscillations (e.g., Trigo et al., 2000). In the western and central zones of Iberia, the North Atlantic Oscillation (NAO), East-Atlantic (EA), and the Scandinavian (SCAND) pattern control precipitation (e.g., Comas-Bru & McDermott, 2014; Trigo et al., 2006). Due to the abrupt topography and Mediterranean Sea climate influences, the westerlies influence decreases towards eastern Iberia (Martín-Vide & Lopez-Bustins, 2006). The elevation and different mountain exposition to the main air masses translate into varying snow timing and magnitudes (Bonsoms, Salvador-Franch, & Oliva, 2021). Consequently, in the Iberian Mountain ranges, snowpacks decrease following a North–South gradient for the same elevation ranges (Alonso-González, López-Moreno, Navarro-Serrano, & Revuelto, 2020; Alonso-González, López-Moreno, Navarro-Serrano, Sanmiguel-Valladolid, et al., 2020).

Several studies have analysed the spatiotemporal distribution of precipitation in Iberia (e.g., De Luis

et al., 2010; Martín-Vide, 1986; Rodríguez-Puebla, Encinas, Nieto & Garmendia, 1998; Trigo et al., 2004) as well as the atmospheric circulation and teleconnection influences (e.g., González-Hidalgo et al., 2009; Martínez-Artigas et al., 2021; Vicente-Serrano & Trigo, 2011). However, the interannual and intra-annual variability of snow accumulation in the Iberian Peninsula Mountain ranges and their climatic controls remain poorly understood. Alonso-González, López-Moreno, Navarro-Serrano, and Revuelto (2020) and Alonso-González, López-Moreno, Navarro-Serrano, Sanmiguel-Valladolid, et al. (2020) analysed the snowpack variability due to NAO for the Iberian ranges, finding a high correlation between snow accumulation and NAO in the southern exposed Iberian Mountain ranges. In the southern slopes of the Pyrenees, NAO negative phases control snow accumulation (López-Moreno, 2005; López-Moreno & Vicente-Serrano, 2007); however, the NAO influence decreases towards the northern and eastern areas (Bonsoms, Salvador-Franch, & Oliva, 2021). In the Pyrenees, the atmospheric circulation variability has been linked to winter precipitation (Lemus-Canovas et al., 2018), snow depth, snow accumulation, and snow days trends in the western and central (López-Moreno, 2005; López-Moreno & Vicente-Serrano, 2007), low elevation southern slopes (Buisan et al., 2015, 2016), eastern (Bonsoms, Salvador-Franch, & Oliva, 2021) and the entire range (López-Moreno et al., 2020). Since 1980s, the positive trend in anticyclonic weather types frequency in spring has been related with the increase of the energy available for snow ablation (Bonsoms et al., 2022).

Long-term snow climatological studies within Iberian Peninsula mountains reveal snow depth decreases attributed to climate warming (López-Moreno et al., 2020) in accordance with Northern Hemisphere snowpack magnitude and snow cover trends (Notarnicola, 2022; Sospedra-Alfonso and Merryfield, 2017). The anticipated increase of temperature is expected to critically affect the future snowpack evolution (Bonsoms et al., 2023; López-Moreno et al., 2011, 2017). Climate projections suggest changes in the frequency distribution of snowfall (López-Moreno et al., 2011) due to thermodynamic (O’Gorman, 2014) and dynamic changes (Faranda, 2019).

However, the frequency concentration of snowfall events in the Iberian Peninsula Mountain ranges during

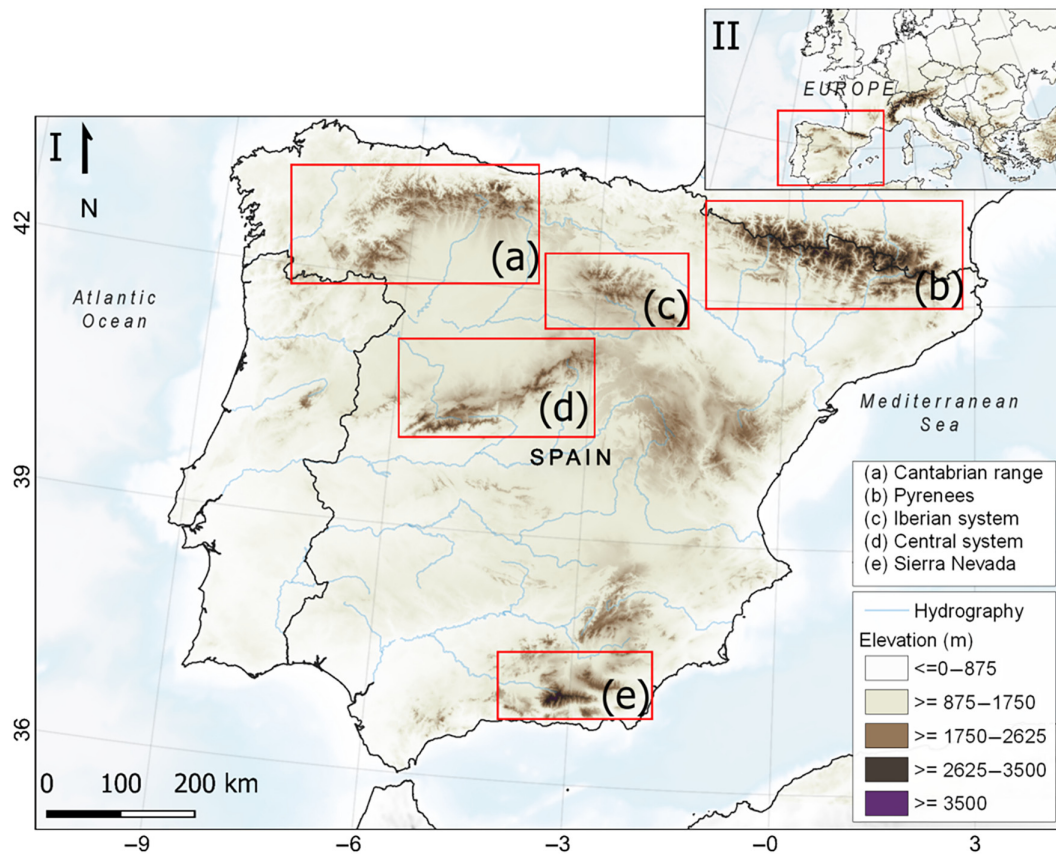


FIGURE 1 (I) Spatial distribution of the Iberian Mountain ranges analysed in this work. (II) Location map of the Iberian Peninsula within the European continent. [Colour figure can be viewed at [wileyonlinelibrary.com](https://onlinelibrary.wiley.com/doi/10.1002/joc.3838)]

the winter season remains poorly understood. For this reason, in this work, we introduce the concentration index (CI; Martin-Vide, 2004) for analysing the intra-seasonal variability of snowfalls in the Iberian Mountain ranges during the 1980–2015 period. The CI takes into consideration the distribution of events throughout the season, displaying high (low) CI values if snow accumulation season is characterized by few (many) accumulation or snowfall events. The CI can be particularly interesting for analysing snowfall data for several reasons: (1) by calculating the CI for snowfall events, we can better understand the seasonal variability of snowfall within a region. This can help identify patterns and trends in snowfall distribution, such as whether snowfall occurs predominantly in a few heavy events or is more evenly distributed throughout the season; (2) analysing the CI for snowfall can help assess the impacts of climate change on snowfall patterns. Changes in the CI over time may indicate shifts in the distribution of snowfall events, which could have implications for water resource management, flood risks, and ecosystem health; (3) Understanding the distribution of snowfall events using the CI can help inform water resource management strategies, particularly in regions where snowmelt is an essential source of water supply.

In this sense, the objectives of this work are:

1. Analyse the spatiotemporal patterns and trends of snowfall temporal concentration in the Iberian Peninsula Mountain ranges.
2. Determine the main geographical and climate drivers of the intra- and inter-annual variability of temporal concentration of snowfalls.

2 | STUDY AREA

The Iberian Peninsula is constituted by an extended plateau (ca. 600 m) located in the middle zone, where the Central system is found (Figure 1). The Iberia Plateau is surrounded by external mountain ranges; including the five mountain ranges analysed in this work, which are, from North to South: the Pyrenees, Cantabrian, Central, Iberian and Baetic system (Sierra Nevada). Maximum elevations are found in Sierra Nevada (Mulhacén, 3478 m a.s.l) and the Pyrenees (Aneto, 3404 m a.s.l), followed by Cantabrian (Torrecerredo, 2648 m a.s.l), Central (2592 m a.s.l, Almanzor Peak), and Iberian range (Moncayo, 2314 m a.s.l). The mean annual average temperature at sea level ranges from 14°C (Cantabrian coastline) to 18°C

(Guadalquivir valley), following a latitudinal gradient approximately of $1^{\circ}\text{C}/200\text{ km}$ (1971–2000 period; De Castro et al., 2005). The abrupt topography decreases the Atlantic influence towards the eastern Iberia, where precipitation is influenced by the Mediterranean climate, showing lower annual amounts and higher annual variability than the western area (Martín-Vide & Olcina, 2001; Martín-Vide and López-Bustins, 2006), reaching an average annual precipitation of $>1000\text{ mm}$ and a CI of 0.71 ($<250\text{ mm}$, $\text{CI} = 0.55$) in the North-West (South-East) Iberia (De Castro et al., 2005). The average max SWE at 1900 m is 471 mm (Cantabrian), 347 mm (Pyrenees), 150 mm (Iberian), 120 mm (Central), and 8.3 mm (Sierra Nevada); whereas the maximum SWE is found during the last weeks of January (Sierra Nevada), February (Central and Iberian) and first week of March (Cantabrian and Pyrenees; 1980–2014 period; Alonso-González et al., 2018).

3 | DATA AND METHODS

3.1 | Snowpack data

In this work, we used the Iberian Peninsula snowpack database generated by Alonso-González et al. (2018). The database provides daily snow depth and Snow Water Equivalent (SWE) estimates for flat surfaces at elevations from 500 to 2900 m (by 100 m intervals) with 0.088° ($\sim 10\text{ km}$) of spatial resolution. The temporal period covers from 1980 to 2014. Snow data were simulated by forcing the physically based Flexible Snow Model (FSM2; Essery, 2015) with ERA-Interim data, dynamically down-scaled using the mesoscale atmospheric model Weather Research and Forecasting. The database was validated using ground-truth snow depth data and remotely sensed imagery, and has been used to analyse the dynamics of the snowpack in previous studies (Alonso-González, López-Moreno, Navarro-Serrano, & Revuelto, 2020; Alonso-González, López-Moreno, Navarro-Serrano, Sanmiguel-Vallelado, et al., 2020). Further details of the methodology followed for the developing of the database and its validation are available at Alonso-González et al. (2018).

3.2 | CI on daily snowfall

The seasonal concentration or irregularity of snowfalls—or snow accumulation—is quantified through the CI index. The CI, introduced by Martín-Vide (2004), is a statistical measure specifically designed to analyse the

distribution and concentration of precipitation events within a given time period for example, winter season. The CI provides a way to quantify the distribution of precipitation events with higher values indicating a more uneven or concentrated distribution, and lower values suggesting a more even distribution of events across the period selected.

The CI calculates the Lorenz curve (Figure 2, curves A and B) which is a graphical representation of the distribution of snowfall events, plotting the cumulative percentage of number of days (X_i) against the cumulative percentage of snowfall (Y_i), with perfect equality represented by a diagonal line, illustrating the concentration of snowfall events within the given time frame. (Figure 2). The resulting frequency distribution clearly shows a negative exponential shape (Martín-Vide, 2004).

It is noted that the area between the equidistribution line and the concentration curves (S) can provide a measure for precipitation irregularity (Martín-Vide, 2004). The Gini index is used to quantify it:

$$\text{Gini's Index} = 2S/10.000 \quad (1)$$

However, the Gini index can be refined by replacing Lorenz or polygonal curves with better fitting exponential curves (Jolliffe & Hope, 1996). Studies by and Martín-Vide (2004) and Riehl (1949) introduced the following calculation procedure for adjustment:

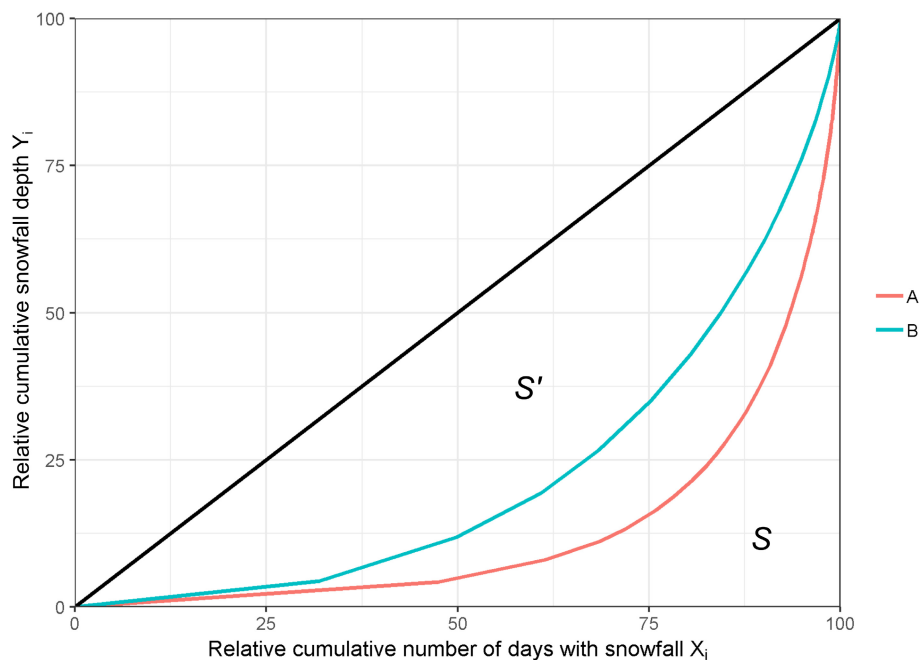
$$Y = aXe^{bx} \quad (2)$$

The constants a and b in Equation (2) can be determined by the least squares method. Once the two constants (a , b) have been determined, the defined integral of the exponential curve between 0 and 100 shows the area between the curve, the x -axis and the y -axis at $y = 100$, which is equivalent to the following:

$$s = \int_0^{100} \left[\frac{a}{b} e^{bx} \left(x - \frac{1}{b} \right) dx \right] \quad (3)$$

As our interest lies in evaluating the irregularity or daily snowfall concentration, that is, the separation with respect to the equidistribution line, we subtracted 5000 (area of the triangle under the equidistribution line) and the value obtained in Equation (3), in order to find the area between the curve, the equidistribution line and the ordinate $Y = 100$ (S'):

FIGURE 2 Comparative CI curve between the relative cumulative snowfall depth and the relative cumulative number of days with snowfall. Curve A represents a time series distribution for a grid point in Eastern Sierra Nevada, whereas B is a time series corresponding for a grid point in northern Pyrenees. The area S' is that delimited by the diagonal equidistribution line and the concentration curve, while the area S is the remaining area below the equidistribution line. [Colour figure can be viewed at [wileyonlinelibrary.com](https://onlinelibrary.wiley.com/doi/10.1002/joc.3838)]



$$S' = 5000 - S \quad (4)$$

With this area, the CI can be defined as follows:

$$CI = S' / 5000 \quad (5)$$

Therefore, the value of the CI is the fraction of S' with respect to the lower triangle delimited by the equidistribution line (Martin-Vide, 2004).

3.3 | Circulation weather types

We performed a principal component analysis (PCA) synoptic classification based on the proposed method by Esteban et al. (2005). This procedure was applied by means of the SynoptReg R package (Lemus-Canovas, Lopez-Bustins, Martín-Vide, & Royé, 2019a). The sea level pressure (SLP) data were obtained from the ERA-5 database (Hersbach et al., 2020) from November to April (included), according to the snow accumulation season. In addition, SLP data were originally hourly and were converted to daily to apply the classification approach. This method was previously applied to the circulation type (CT) classification of precipitation events (e.g., Lemus-Canovas et al., 2018; 2019b) or snow accumulation (e.g., Bonsoms, Salvador-Franch, & Oliva, 2021), among other works. After running the PCA, we selected five PC components explaining most of the variance of the original data (87.5%) by conducting a Scree Test (Cattell, 1966). These PCs were subsequently rotated by means of a varimax rotation (Esteban et al., 2006). With the rotated components, we used the scores to apply the

extreme scores method (Esteban et al., 2005). The scores show the degree of representativeness associated with the variation modes of each principal component, that is, the classification of each day to its more representative centroid. Thus, the extreme scores method uses the scores >2 and <-2 , establishing a positive and negative phase for each principal component. The extreme scores procedure establishes the number of groups and their centroids for the K-means method (Esteban et al., 2006). K-means is applied without iterations because the centroids are well established by the method of extreme scores. This procedure culminates in a 10 CT classification. The CT classification was performed between 30° N– 60° N and 30° W– 20° E, with a 0.25° grid resolution.

3.4 | Low-frequency climate modes

We performed a person's correlation between the annual CI value and the different low-frequency climate modes that rule the atmospheric variability in Iberia. The teleconnection patterns included in this work are the NAO (Hurrell, 1995), the EA pattern (Wallace & Gutzler, 1981), East-Atlantic/Western Russia pattern (EAWR; Barnston & Livezey, 1987), the SCAND pattern (Barnston & Livezey, 1987), the Mediterranean Oscillation (MO; Conte et al., 1989), and the WeMO (Martin-Vide & Lopez-Bustins, 2006). The NAO is calculated by the difference of SLP in Reykjavik (Iceland) and Ponta Delgada (Azores). The EA pattern is based on a north–south dipole over the North Atlantic Ocean, with the centres of action in a southern position than the

NAO. The EAWR positive phases represent negative SLP anomalies in the North Caspian and positive anomalies in Eurasia. The SCAND oscillation is constituted by a negative centre of action over western Europe and positive SLP anomalies over Scandinavia. The MO is defined as the normalized 500 hPa geopotential heights difference between Algiers (Algeria) and Cairo (Egypt) quantifying a dipolar behaviour of the atmosphere between the Western and Eastern Mediterranean. WeMO negative phases represent negative SLP anomalies over the western Mediterranean Sea. The NAO, MO, and WeMO indexes were downloaded at the Climate Research Unit, University of East Anglia data portal (<https://crudata.uea.ac.uk/cru/data/pci.htm>, 1 May 2023). The EA, EAWR, and SCAND data are provided by the National Center for Atmospheric Research (NCAR; <https://www.cpc.ncep.noaa.gov/data/teledoc/teleintros.html>).

3.5 | Temporal tendency

Here, we analysed the temporal trends computing a linear regression, which constitutes one of the most used approaches for hydroclimatological purposes. Trends were considered statistically significant when the p -value was ≤ 0.1 .

3.6 | Geographical dependence analysis

The Partial Dependence (Greenwell, 2017) analysis was executed using an linear regression to investigate the dependence on the following geographical factors (predictors): elevation, longitude, latitude, Euclidean distance from the Atlantic and Mediterranean coastline, and continentality. For this latest predictor, continentality was calculated as a function of Euclidean distances from the sea to each target raster cell. Partial dependence plots are low-dimensional graphical renderings of the prediction function so that the relationship between the outcome and predictors of interest can be more easily understood (Greenwell, 2017). Each predictor's contribution to the model is quantified by its coefficient, and the significance of these coefficients is evaluated using the t -statistic. The t -statistic gives us a measure of confidence that each predictor variable has a statistically significant impact on the dependent variable.

4 | RESULTS AND DISCUSSION

We introduce the CI for the spatiotemporal analysis of interannual snowfall variability and related trends in the Iberian Peninsula mountain ranges (1980–2015 period).

Additionally, we identify the geographical and low-frequency modes that control the CI by performing a partial dependence analysis based on a multiple linear regression. Finally, we investigate the atmospheric circulation governing the snow CI variability.

4.1 | CI spatiotemporal patterns and trends

The CI shows clear differences depending on the Iberian range analysed and also when different sectors of each mountain range are compared (Figure 3). Snow accumulation is regularly distributed (lower CI values) through the season in the Iberian, Cantabrian, western Sierra Nevada, northern and western slopes of the Central System and Pyrenean ranges. On the contrary, CI markedly increases eastward in the Pyrenees and Sierra Nevada, zones clearly influenced by Mediterranean climate.

An elevation dependence can also be visually determined in the CI values. The higher the elevation, the lower the CI. A more extended review about geographical factors determining CI spatial patterns is exposed in Section 4.3.

4.2 | Synoptic circulation drivers and temporal trends of CI

The CT classification conducted in this work identifies 10 synoptic configurations that govern atmospheric patterns from November to April (Figure 4). Based on Figure 5, CT 1 (698 days), CT 5 (631), CT 7 (488), and CT 10 (587) are Atlantic low-pressure systems. During CT 1, a high-pressure system is located in the subtropical area, near the Azores, while a westward advection of maritime and polar air masses brings cold and wet conditions over the Iberian Peninsula. CT 1 is the most recurrent CT in November (Figure 5). CT5 is mainly characterized by a deep low-pressure system placed in the North Atlantic sector, advecting western and southwestern maritime wet air masses specially to the northwestern part of the Iberian Peninsula. Additionally, under this CT5, the southern and eastern part of the Iberian Peninsula are more affected by the subtropical ridge arising from the south, therefore restricting the above-mentioned wet conditions to the western and northwestern mountain ranges of the study area. During CT 7 events, a deep low-pressure system is located just northwest of the Iberian Peninsula. This synoptic pattern is the most frequent in April (24% of the days) and is characterized by southwestward advection of maritime, mild, and wet flows, providing substantial precipitation episodes.

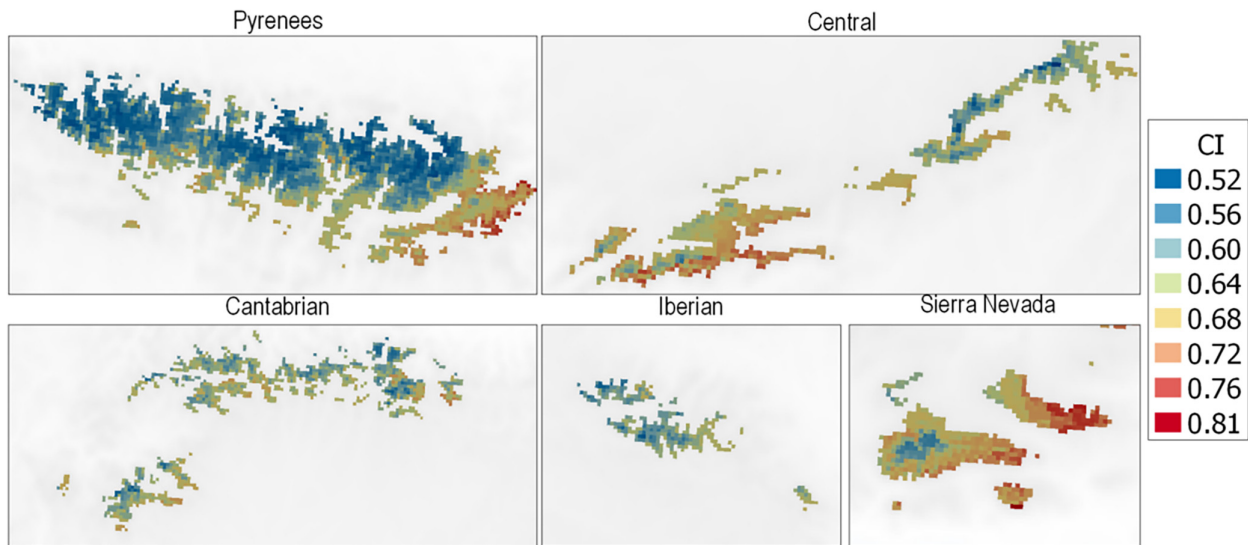
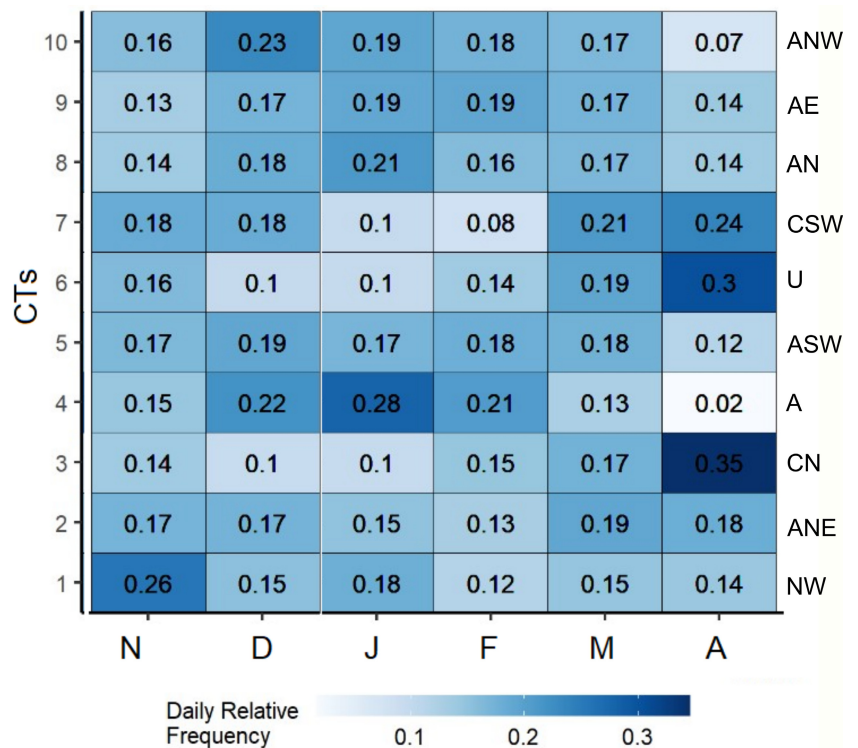


FIGURE 3 Spatial distribution of the concentration index through the Iberian Peninsula Mountain ranges. [Colour figure can be viewed at wileyonlinelibrary.com]

FIGURE 4 Daily relative frequency of each circulation type (CT) grouped by month of the snow season. The right-hand side shows the acronyms related to each weather type. “A” and “C” refers to anticyclonic and cyclonic types, respectively. [Colour figure can be viewed at wileyonlinelibrary.com]



Finally, CT 10 brings a polar advection of cold northwest air masses.

CT 2 (601), CT 3 (601), CT 6 (578), and CT 8 (562) form a second cluster of atmospheric configurations characterized by Mediterranean wet air mass advectons origin. During CT 2, an anticyclonic system is extended in the north of the Iberian Peninsula. In contrast, during CT 8, the high-pressure area is located just southwest of the Iberian Peninsula. In both CTs, weak western

Mediterranean advection of northeast and north wet air flows may bring precipitation. Similarly, CT 3 is defined by a weakened anticyclone in the southwest Iberian Peninsula and a low placed in northern Italy, triggering north and northeast advection of wet Mediterranean air flow, being highly frequent during the last month of the season when it is recorded for the majority of the days (35%). Finally, CT 6 is characterized by a high-pressure system displaced towards Western Europe, providing

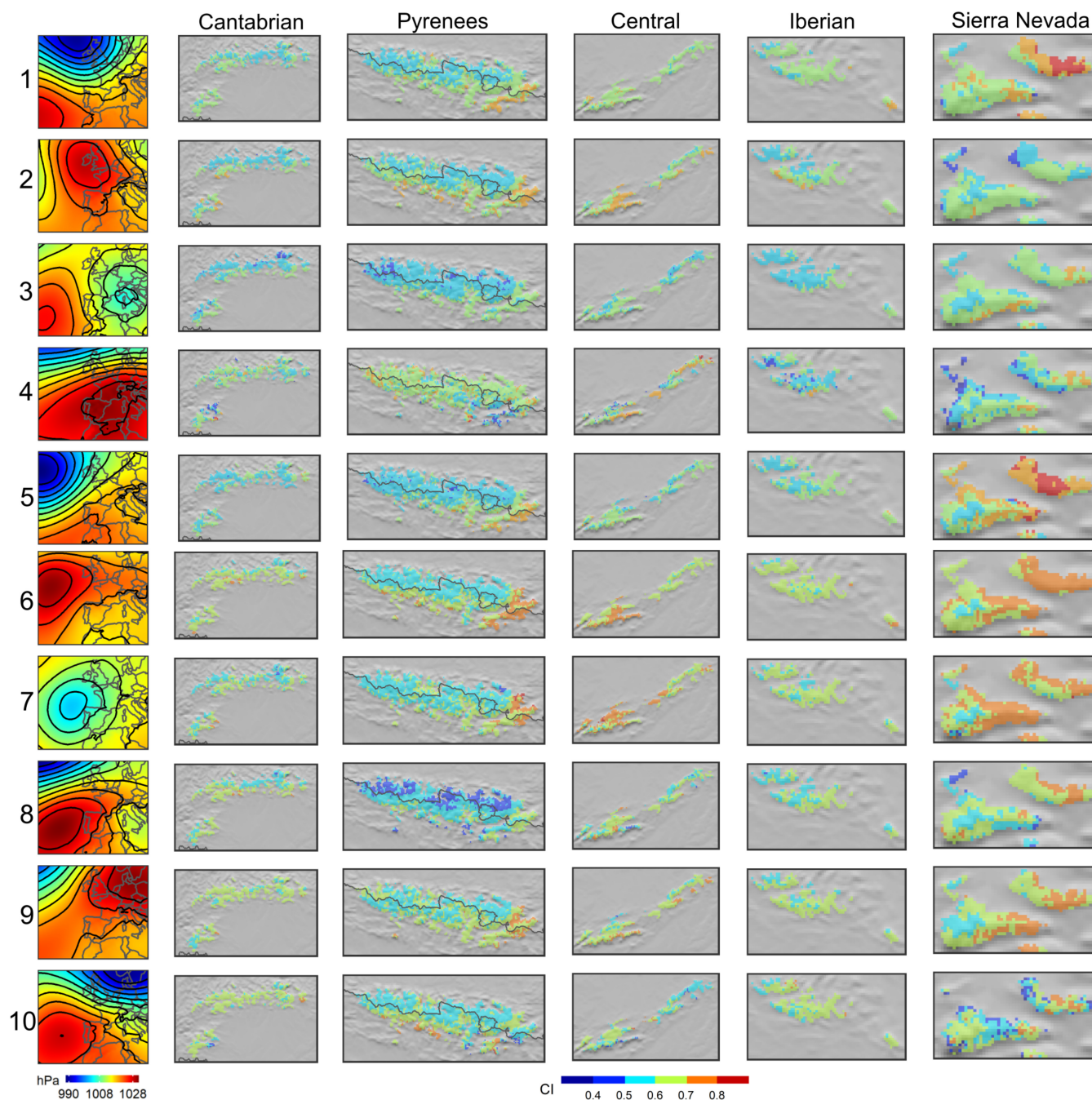


FIGURE 5 Spatial map of the average concentration index (CI) for each circulation types (CTs), grouped by mountain ranges. The average sea level pressure pressure (in hPa) during each CTs is shown in the left column. [Colour figure can be viewed at wileyonlinelibrary.com]

stable weather—undefined situation in the circulation—in combination with mild conditions over the Iberian mountains.

The synoptic configurations comprised of CT 4 (702), CT 8, and CT 9 (775) bring high-pressure systems and stable weather over the Iberian Peninsula. CT 4 rarely triggers snow accumulation events, being highly frequent during January (28% of the days). During CT 8, the extension of an anticyclone system in the west and southwest

Iberian Peninsula provides very stable weather in the western sector. However, eastern Iberia is under the influence of Mediterranean cyclogenesis, which could trigger snowfall events in the highlands. Finally, CT 9 is a stationary-cold continental high-pressure system established over central Europe that brings dry conditions over the Iberian Peninsula.

The Cantabrian range presents moderate CI values and a relatively constant CI, independent of the CT

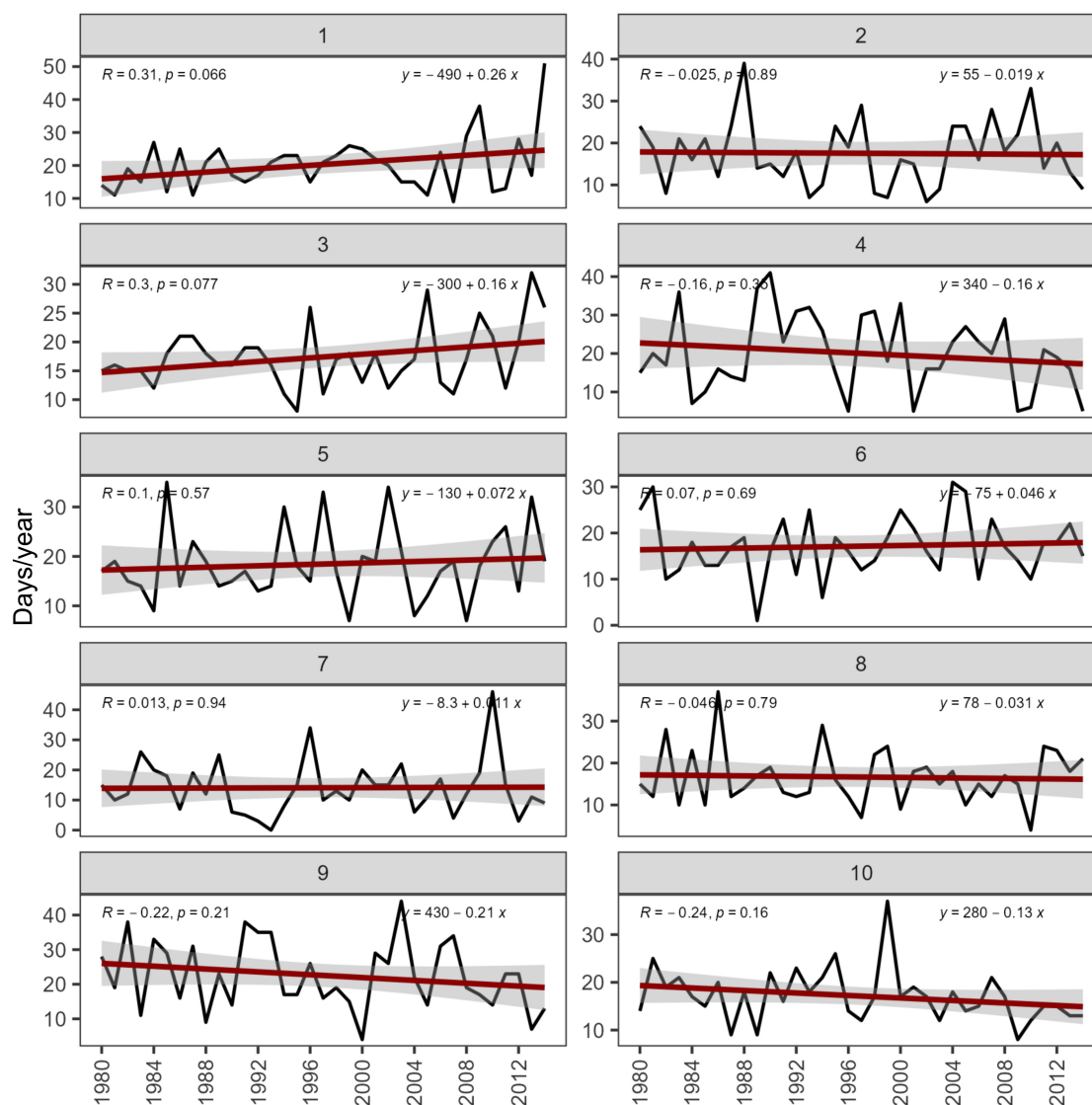


FIGURE 6 Temporal evolution of the circulation types daily frequency per snow season. [Colour figure can be viewed at wileyonlinelibrary.com]

group. This mountain range is exposed to polar and maritime Atlantic cold low-pressure systems (CT 1 and CT 5), allowing a regular distribution of snow accumulation events during the snow season. The northern and southern Pyrenees show a contrasting CI pattern. The northern slopes are exposed to low CI values. This is explained because the majority of CTs (except anticyclonic, CT4) could trigger snow accumulation events due to the high exposure of the mountain range to the Atlantic but also Mediterranean low-pressure systems (north and northeast advections). The maximum CI values are precisely related to CT 4 events, which bring stable conditions and snow ablation. CT 3 (cyclonic north advection) triggers high rainfall episodes (Esteban et al., 2009; Lemus-Canovas, Lopez-Bustins, Trapero, & Martin-Vide, 2019b) and large snow accumulation events in the windward

and northern Pyrenees (Bonsoms, Salvador-Franch, & Oliva, 2021), decreasing towards the leeward and southern slopes of the range, where greater values are reached (CI = 0.7 and 0.8).

The Central range presents CI values around 0.5. The greatest values (CI = 0.7) are found in the eastern sector under CT 2 (anticyclonic northeast advection) and in the western, Atlantic-influenced area under CT 7 (cyclonic southwest advection). The Iberian range presents CI values around 0.6 and does not show significant differences under the different synoptic types. In Sierra Nevada, however, there are large differences depending on the synoptic episode. Data reveal that the western area rainshadows the eastern sector under CT 1, CT 5, and CT 7 (westerly advections). In the eastern (western) zone, the maximum (minimum) CI values are observed during the

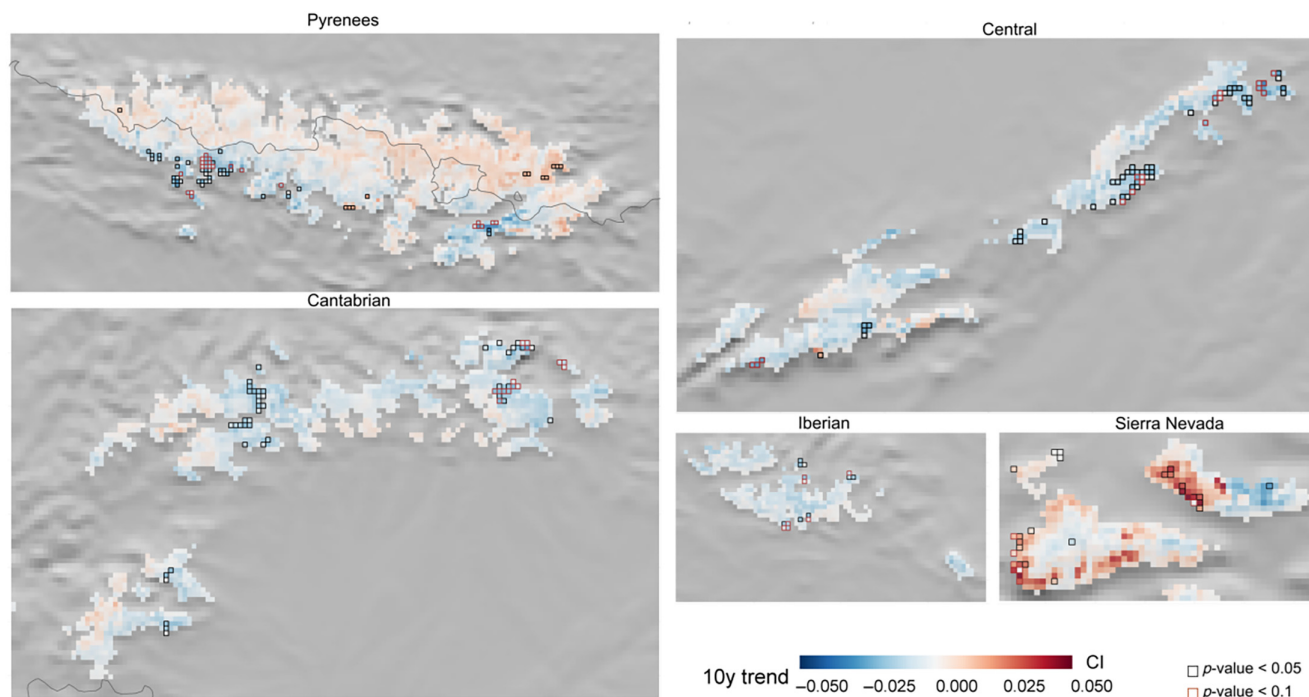


FIGURE 7 Spatial concentration index trends for the Iberian Mountain ranges are included in this work. [Colour figure can be viewed at wileyonlinelibrary.com]

latter synoptic configurations, whereas the minimum values are observed during Mediterranean low-pressure systems (CT 3 and CT 8). Those results are consistent with the contrasted rain patterns found between the western and eastern areas of the range (Pereira et al., 2016).

The synoptic evolution during the temporal period analysed shows no significant change in the daily frequency for CT 2, CT 7, and CT 8 (Figure 6). There is a general decrease of anticyclonic CTs (CT 9, CT 4, and CT 10), and an increase of low-pressure systems. In detail, there is a statistically significant increase in the daily frequency of CT 1 and CT 3 (0.16/year, p -value < 0.1). The upward trend found for these synoptic events seems to explain the general decrease of CI found in the eastern exposed Iberian Peninsula ranges (Figure 7). In addition to the orientation, there is also a partial altitudinal gradient in the increase of the CI for Sierra Nevada (Figure 7), which could be related to a lower number of snowfall days, due to the global temperature increase and the phase change that this implies in precipitation (Pérez-Palazón, Pimentel & Polo, 2018). In the other hand, stable situations as CT 4 and CT 9 that rarely triggers snow accumulation events showed a non-statistically significant decreasing trend (slope = -0.16 /year and -0.21 , respectively, p -value > 0.1; Figure 6), but favouring less snowfall events and promoting and increase of CI values, especially in those areas where the CI was historically lower as the northern part of the Pyrenees. Conversely,

the south and southwestern parts of the Pyrenees observe a statistically significant trend towards the reduction of the CI, probably triggered by a statistically significant increase in the frequency of CT 1, as it provides moisture from westerly flows to this area, resulting in more regular snowfalls.

4.3 | Geographical and low-frequency climate modes driving spatial behaviour of CI

The contribution of each independent variable is evaluated through the t -statistic. The most relevant predictor for the CI estimation is elevation ($t = 42$; Figure 8a) followed by the Atlantic distance ($t = 30$; Figure 8a). Interestingly, in Figure 9a elevation shows an inverse relationship with CI—the greater the elevation, the lower the CI—whereas the Atlantic distance shows a positive relationship, being those areas close to the Atlantic those with a less snowfall concentrations—lower CI. In this sense, Figure 8b summarize the abovementioned: higher elevations in the mountain systems close to the Atlantic are those with a lesser CI, while the low elevations of the mountain systems further away from the Atlantic are those with the highest CI.

The Atlantic distance is the driver of CI since it indirectly expresses the mountain exposure to the main

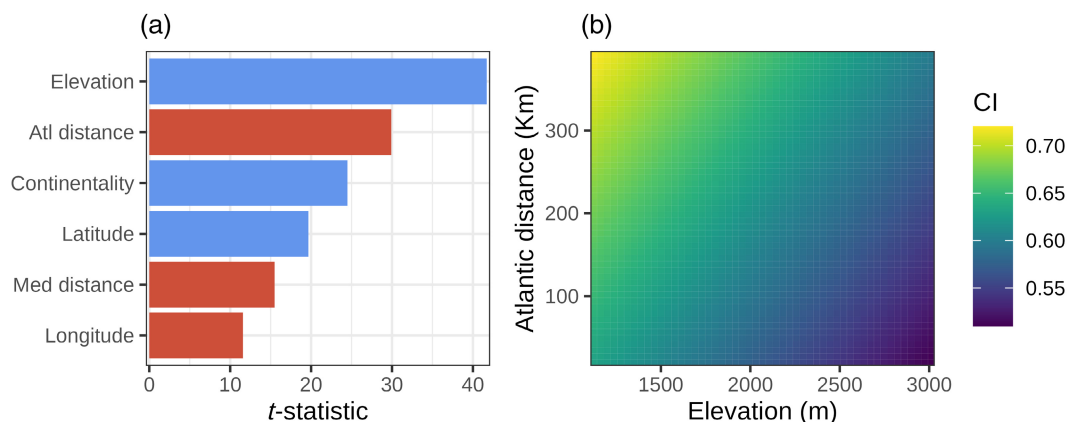


FIGURE 8 Partial dependence analysis of the concentration index (CI) and the geographical predictor variables. (a) *t*-Statistic performance of the geographical variables included in the model. Blue and red colours show an inverse or direct relationship between CI and the geographical factors, respectively. (b) Relationship between Atlantic distance and elevation. The colour gradient indicates the values of the CI with respect to these two variables. [Colour figure can be viewed at [wileyonlinelibrary.com](https://onlinelibrary.wiley.com/doi/10.1002/joc.3838)]

circulation weather types that trigger snow accumulation during the cold half of the year (N, NW, W advections). The latter synoptic configurations are linked to snow accumulation events in the northern Iberian Peninsula, such as the Cantabrian and Pyrenees Mountain ranges (Esteban et al., 2005). The relationship of CI with elevation is consistent with high values of the coefficient of variation (CV) detected at low-elevation sectors in contrast to highlands of the Iberian Peninsula mountain ranges Alonso-González, López-Moreno, Navarro-Serrano, & Revuelto, 2020; Alonso-González, López-Moreno, Navarro-Serrano, Sanmiguel-Vallelado, et al., 2020). This greater variability at lower elevations could also be related to a lower number of snowfalls due to the temperature gradient. Few snowfalls represent the total snow accumulation of the whole season. Furthermore, the link between CI and the distance to the Atlantic Ocean is consistent with Iberian Peninsula rainfall patterns. Rainfall interannual variability decreases (increases) towards the North and West (South and East) sectors of the Iberian Peninsula (Martín-Vide et al., 2022).

The CI spatial behaviour in the Iberian Peninsula allows us to relate the different geographical factors distinguished above with the main teleconnections that drive precipitations in the study area. However, the links of each teleconnection pattern and CI show different correlations depending on each sector of the mountain range (Figure 9). The exposure of the mountain range to the dominant airflow in each phase of each teleconnection is a very relevant factor in explaining the spatial distribution of the correlation between the annual CI and each teleconnection index. NAO and EAWR act with similar patterns in the Cantabrian, Pyrenees, and Iberian mountains, showing a positive relationship between the

circulation indices and the CI. The highest correlation values are related to their southern or southwestern parts due to the influence of Atlantic air masses. These indices tend to increase the CI values during their dry phases when snowfall events are temporally discontinuous. On the contrary, during their negative phases, these indices tend to promote more regular precipitation from the Atlantic with W and SW surface flows, triggering more temporally distributed snowfalls in the aforementioned mountain regions, especially in their western and southwestern slopes. The largest correlations found in these ranges are potentially explained by the west-to-east disposition of most of the Iberian range. Mountain orographic barriers and rain shadow effects explain the differences observed between the northern-southern slopes of the Pyrenees and western-eastern Sierra Nevada (Figure 3).

For the Pyrenees, CI values are consistent with the different snow accumulation and timing patterns found in the range (Bonsoms, Gonzalez, et al., 2021; Buisan et al., 2016; López-Moreno & Vicente-Serrano, 2007; Navarro-Serrano and López-Moreno, 2017). Positive (negative) WeMO phases are linked with low (high) CI values in the northern Pyrenees. WeMO positive phases are related to N, NW, and WNW wet and cold advections (Martín-Vide and López-Bustins, 2006). In the western and central areas of the southern slopes of the Pyrenees, negative (positive) NAO phases show a low (high) link with CI. Negative NAO values drive a SW wet and mild airflow over the Iberian Peninsula, whereas positive NAO values are linked with warm air masses and anticyclonic, stable conditions (e.g., Trigo et al., 2006). Snowfalls in the western and central southern slopes of the range are linked with negative NAO oscillations, which is consistent with snow accumulation patterns found in

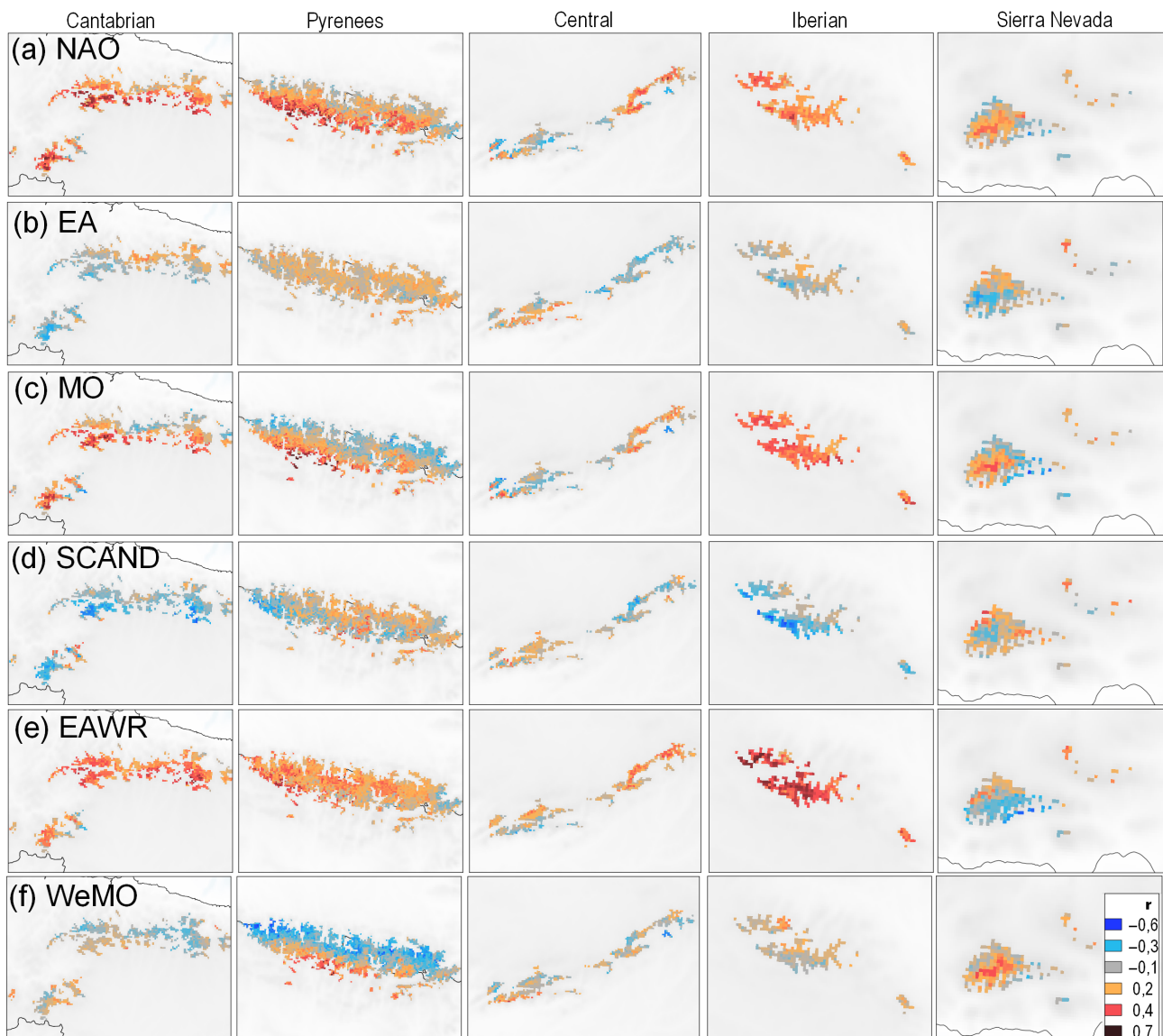


FIGURE 9 Pearson's correlation of the low-frequency climate modes and the Iberian mountain ranges CI. EA, East-Atlantic; EAWR, East-Atlantic/Western Russia; MO, Mediterranean Oscillation; NAO, North Atlantic Oscillation; SCAND, Scandinavian; WeMO, Western Mediterranean Oscillation. [Colour figure can be viewed at wileyonlinelibrary.com]

the range ($r = -0.6$; López-Moreno, 2005; 2011). There is no unique teleconnection pattern that explains the CI variability in the eastern Pyrenees. The highest CI correlations are found with positive SCAND phases in specific massifs of the central area. Positive SCAND phases are linked with Atlantic NW, W, and SW advections (Vicente-Serrano et al., 2006) due to positive high-pressure systems on the Scandinavian Peninsula. Moving southward, there is a slight increase in the NAO and MO correlation, which is in accordance with the low influence of snow accumulation of NAO towards the northern massifs of the Pyrenees (Alonso-González, López-Moreno, Navarro-Serrano, & Revuelto, 2020; Alonso-González, López-Moreno, Navarro-Serrano, Sanmiguel-

Vallado, et al., 2020). This is because the southern massifs of the range are mainly exposed to W and SW airflows. The same results are observed in the southern massifs of the Cantabrian and Iberian ranges, as well as in the Southwest Mountain range, Sierra Nevada.

Circulation dynamics control the spatial variability found in the Central system, which is also observed for the teleconnection patterns. Several teleconnection patterns rule the CI variability over the entire Central system, which is consistent with the different synoptic control (Figure 5). The northern slopes of the eastern sector are controlled by positive NAO and EAWR patterns, whereas the western area shows a clear North–South difference, and no single low-frequency climate mode

dominates the CI variability. Sierra Nevada is primarily controlled by positive WeMO, MO, and NAO phases, which is consistent with winter precipitation being mainly related to these three teleconnections in SE Andalusia (Halifa-Marín et al., 2021).

5 | CONCLUSIONS

In this study, we employed the CI to assess the spatiotemporal patterns of intra-annual daily snow accumulation and its interannual variability during the 1980–2014 period in the Iberian Peninsula mountain ranges. Our findings allowed us to quantify which areas of the mountain systems have their seasonal snowpack built up by a few irregular snowfalls, or whether it is constituted by several snowfalls, more regularly spread over the winter season. The influence of geographical factors and atmospheric circulation patterns on CI variability and provided evidence of the contrasted interannual variability of snow accumulation within Iberian mountain ranges. The main conclusions of this study are:

1. The elevation and the Atlantic ocean distance are the most influential geographical factors of the spatial variability of snowfall concentration during a winter season. The lowest CI values are detected in the northern mountain sectors exposed to Atlantic and Mediterranean northern advections, linked to more regular snowfalls during the snow season. Minimum CI values are found in the northern slopes of the Pyrenees (CI = 0.5) followed by Cantabrian and Iberian range (CI = 0.56). On the other hand, rain-shadow effects and a lower number of events explain the increase of CI towards eastern, Mediterranean-exposed mountain ranges. Here, the maximum CI values are found in the eastern Pyrenees (CI = 0.77) and Sierra Nevada (CI = 81), where snow accumulation is majorly concentrated due to a few episodes during the snow season.
2. Different CI timing and patterns are translated into distinct trends. The CI temporal evolution (1980–2014 period) revealed non-statistically significant increases in CI for the northern slopes of the Pyrenees and decreases in CI for most of the Iberian mountain ranges, especially for Central system and Cantabrian ranges. These trends are in line with the decrease of anticyclonic CTs and the increase of low-pressure systems during the analysed period. In the southernmost mountain range, Sierra Nevada, an increase of CI was observed in low-lands of the range, probably related to an increase of liquid precipitation against a reduction of solid events.

3. CI variability in the Iberian Peninsula mountain ranges is highly controlled by NAO, and EAWR phases, as well as Western Mediterranean Oscillation (WeMO) oscillations in driving the Pyrenees and Sierra Nevada snowfalls concentration. Positive (negative) phases of NAO and EAWR implied dry (wet) and more discontinuous (continuous) snowfalls in the western/southwestern oriented mountain ranges of the mid-north of the Iberian Peninsula, promoting an increase (decrease) of the CI. Mediterranean oscillations as MO and WeMO controlled north/south patterns in the Pyrenees, negative WeMO and MO values promote greater values of CI for the northern part, and vice versa for the southern part.

In view of the presented results, it is necessary to continue investigating the concentration of these snowfalls, especially in relation to the climate change scenarios projected for the coming decades, which may alter the occurrence of such snowfalls and therefore compromise the final management of the hydrological resources provided for the Iberian mountain systems.

AUTHOR CONTRIBUTIONS

Marc Lemus-Canovas: Conceptualization; methodology; investigation; data curation; formal analysis; visualization; writing—original draft; writing—review and editing. **Esteban Alonso-González:** Data curation; investigation; conceptualization; methodology; writing—original draft. **Josep Bonsoms:** Data curation; visualization; writing—original draft; writing—review and editing. **Juan I. López-Moreno:** Supervision; writing—review and editing.

ACKNOWLEDGEMENTS

This work frames within the research topics examined by the research group, MARGISNOW (PID2021-124220OB-I00) funded by the Spanish Ministry of Science and Innovation. M.L.-C. is supported by a postdoctoral contract from the programme named “Programa de axudas de apoio á etapa inicial de formación posdoutoral (2022)” founded by Xunta de Galicia (Government of Galicia, Spain). Reference number: ED481B-2022-055. J.B. is supported by a pre-doctoral University Professor FPI grant (PRE2021-097046) funded by the Spanish Ministry of Science, Innovation and Universities.

DATA AVAILABILITY STATEMENT

The snow depth daily data used in this article are available at <https://zenodo.org/records/854619>. ERA5 data are provided by the Climate Data Store of Copernicus at <https://cds.climate.copernicus.eu/cdsapp#!/dataset/reanalysis-era5-single-levels?tab=overview>. NAO, MO, and

WeMO teleconnection indices are stored in <https://crudata.uea.ac.uk/cru/data/pci.htm>. Whereas EA, EAWR, and SCAND are available at <https://www.cpc.ncep.noaa.gov/data/teledoc/teleintros.html>. The R programming function for computing the Concentration Index (CI) is available upon request.

ORCID

Juan I. López-Moreno  <https://orcid.org/0000-0002-7270-9313>

REFERENCES

- Adam, J.C., Hamlet, A.F. & Lettenmaier, D.P. (2009) Implications of global climate change for snowmelt hydrology in the twenty-first century. *Hydrological Processes*, 23, 962–972. Available from: <https://doi.org/10.1002/hyp.7201>
- Alonso-González, E., López-Moreno, J.I., Gascoin, S., García-Valdecasas Ojeda, M., Sanmiguel-Valladolid, A., Navarro-Serrano, F. et al. (2018) Daily gridded datasets of snow depth and snow water equivalent for the Iberian Peninsula from 1980 to 2014. *Earth System Science Data*, 10, 303–315. Available from: <https://doi.org/10.5194/essd-10-303-2018>
- Alonso-González, E., López-Moreno, J.I., Navarro-Serrano, F., Sanmiguel-Valladolid, A., Revuelto, J., Domínguez-Castro, F. et al. (2020) Snow climatology for the mountains in the Iberian Peninsula using satellite imagery and simulations with dynamically downscaled reanalysis data. *International Journal of Climatology*, 40, 477–491. Available from: <https://doi.org/10.1002/joc.6223>
- Alonso-González, E., López-Moreno, J.I., Navarro-Serrano, F.M. & Revuelto, J. (2020) Impact of North Atlantic oscillation on the snowpack in Iberian Peninsula mountains. *Water*, 12(1), 105. Available from: <https://doi.org/10.3390/w12010105>
- Barnston, A.G. & Livezey, R.E. (1987) Classification, seasonality, and persistence of low Frequency atmospheric circulation patterns. *Monthly Weather Review*, 115, 1083–1126. Available from: [https://doi.org/10.1175/1520-0493\(1987\)115<1083:CSAPOL>2.0.CO;2](https://doi.org/10.1175/1520-0493(1987)115<1083:CSAPOL>2.0.CO;2)
- Bonsoms, J., Gonzalez, S., Prohom, M., Esteban, P., Salvador-Franch, F., López-Moreno, J.I. et al. (2021) Spatio-temporal patterns of snow in the Catalan Pyrenees (NE Iberia). *International Journal of Climatology*, 41(12), 5676–5697. Available from: <https://doi.org/10.1002/joc.7147>
- Bonsoms, J., López-Moreno, J.I. & Alonso-González, E. (2023) Snow sensitivity to temperature and precipitation change during compound cold-hot and wet-dry seasons in the Pyrenees. *The Cryosphere*, 17(3), 1307–1326. Available from: <https://doi.org/10.5194/tc-17-1307-2023>
- Bonsoms, J., López-Moreno, J.I., González, S. & Oliva, M. (2022) Increase of the energy available for snow ablation and its relation with atmospheric circulation. *Atmospheric Research*, 275, 106228. Available from: <https://doi.org/10.1016/j.atmosres.2022.106228>
- Bonsoms, J., Salvador-Franch, F. & Oliva, M. (2021) Snowfall and snow cover evolution in the eastern pre-pyrenees (NE Iberian peninsula). *Geographical Research Letters*, 47(2), 291–307. Available from: <https://doi.org/10.18172/cig.4879>
- Buisan, S.T., López-Moreno, J.I., Saz, M.A. & Kochendorfer, J. (2016) Impact of weather type variability on winter precipitation, temperature and annual snowpack in the Spanish Pyrenees. *Climate Research*, 69, 79–92. Available from: <https://doi.org/10.3354/cr01391>
- Buisan, S.T., Saz, M.A. & López-Moreno, J.I. (2015) Spatial and temporal variability of winter snow and precipitation days in the western and central Spanish Pyrenees. *International Journal of Climatology*, 35(2), 259–274. Available from: <https://doi.org/10.1002/joc.3978>
- Cattell, R.B. (1966) The scree test for the number of factors. *Multivariate Behavioral Research*, 1(2), 245–276.
- Chen, X., An, S., Inouye, D.W. & Schwartz, M.D. (2015) Temperature and snowfall trigger alpine vegetation green-up on the world's roof. *Global Change Biology*, 21(10), 3635–3646. Available from: <https://doi.org/10.1111/gcb.12954>
- Comas-Bru, L. & McDermott, F. (2014) Impacts of the EA and SCA patterns on the European twentieth century NAO-winter climate relationship. *Quarterly Journal of the Royal Meteorological Society*, 140, 354–363. Available from: <https://doi.org/10.1002/qj.2158>
- Conte, M., Giuffrida, A. & Tedesco, S. (1989) *The Mediterranean oscillation. Impact on precipitation and hydrology in Italy*. Helsinki: Publications of the Academy of Finland.
- De Castro, M., Martín-Vide, J. & Alonso, S. (2005) *El clima de España: pasado, presente y escenarios de clima para el siglo XXI. En Impactos del cambio climático en España*. Madrid: Ministerio Medio Ambiente, p. 64.
- De Luis, M., Brunetti, M., Gonzalez-Hidalgo, J.C., Longares, L.A. & Martín-Vide, J. (2010) Changes in seasonal precipitation in the Iberian Peninsula during 1946–2005. *Global and Planetary Change*, 74, 27–33.
- Essery, R. (2015) A factorial snowpack model (FSM 1.0). *Geoscientific Model Development*, 8(12), 3867–3876. Available from: <https://doi.org/10.5194/gmd-8-3867-2015>
- Esteban, P., Jones, P.D., Martín-Vide, J. & Mases, M. (2005) Atmospheric circulation patterns related to heavy snowfall days in Andorra, Pyrenees. *International Journal of Climatology*, 25(3), 319–329. Available from: <https://doi.org/10.1002/joc.1103>
- Esteban, P., Martín-Vide, J. & Mases, M. (2006) Daily atmospheric circulation catalogue for western Europe using multivariate techniques. *International Journal of Climatology*, 26, 1501–1515. Available from: <https://doi.org/10.1002/joc.1391>
- Esteban, P., Ninyerola, M. & Prohom, M. (2009) Spatial modelling of air temperature and precipitation for Andorra (Pyrenees) from daily circulation patterns. *Theoretical and Applied Climatology*, 96, 43–56. Available from: <https://doi.org/10.1007/s00704-008-0035-3>
- Faranda, D. (2019) An attempt to explain recent trends in European snowfall extremes. *Weather and Climate Dynamics*, 1, 445–458. Available from: <https://doi.org/10.5194/wcd-1-445-2020>
- Fayad, A., Gascoin, S., López-Moreno, J.I., Drapeau, L., Le Page, M. & Escadafal, R. (2017) Snow hydrology in Mediterranean Mountain regions: a review. *Journal of Hydrology*, 42, 374–396. Available from: <https://doi.org/10.1016/j.jhydrol.2017.05.063>
- González-Hidalgo, J.C., Lopez-Bustins, J.A., Stepanek, P., Martín-Vide, J. & de Luis, M. (2009) Monthly precipitation trends on the Mediterranean fringe of the Iberian Peninsula during the

- second-half of the twentieth century (1951–2000). *International Journal of Climatology*, 29, 1415–1429.
- Greenwell, B.M. (2017) Pdp: an R package for constructing partial dependence plots. *The R Journal*, 9(1), 421–436. Available from: <https://doi.org/10.32614/RJ-2017-016>
- Halifa-Marín, A., Lorente-Plazas, R., Pravia-Sarabia, E., Montávez, J.P. & Jiménez-Guerrero, P. (2021) Atlantic and Mediterranean influence promoting an abrupt change in winter precipitation over the southern Iberian Peninsula. *Atmospheric Research*, 253, 105485. Available from: <https://doi.org/10.1016/J.ATMOSRES.2021.105485>
- Hersbach, H., Bell, B., Berrisford, P., Hirahara, S., Horányi, A., Muñoz-Sabater, J. et al. (2020) The ERA5 global reanalysis. *Quarterly Journal of the Royal Meteorological Society*, 146, 1999–2049. Available from: <https://doi.org/10.1002/qj.3803>
- Hurrell, J.W. (1995) Decadal trends in the North Atlantic oscillation: regional temperatures and precipitation. *Science*, 269, 676–679. Available from: <https://doi.org/10.1126/science.269.5224.676>
- Joliffe, I.T. & Hope, P.B. (1996) Representation of daily rainfall distributions using normalized rainfall curves. *International Journal of Climatology*, 16, 1157–1163. Available from: [https://doi.org/10.1002/\(SICI\)1097-0088\(199610\)16:10<1157::AID-JOC71>3.0.CO;2-R](https://doi.org/10.1002/(SICI)1097-0088(199610)16:10<1157::AID-JOC71>3.0.CO;2-R)
- Kreyling, J. & Henry, H.A.L. (2011) Vanishing winters in Germany: soil frost dynamics and snow cover trends, and ecological implications. *Climate Research*, 46(3), 269–276. Available from: <https://doi.org/10.3354/cr00996>
- Lemus-Canovas, M. (2022) Changes in compound monthly precipitation and temperature extremes and their relationship with teleconnection patterns in the Mediterranean. *Journal of Hydrology*, 608, 127580. Available from: <https://doi.org/10.1016/J.JHYDROL.2022.127580>
- Lemus-Canovas, M., Lopez-Bustins, J.A., Martín-Vide, J. & Royé, D. (2019a) synoptReg: an R package for computing a synoptic climate classification and a spatial regionalization of environmental data. *Environmental Modelling & Software*, 118, 114–119. Available from: <https://doi.org/10.1016/j.envsoft.2019.04.006>
- Lemus-Canovas, M., Lopez-Bustins, J.A., Trapero, L. & Martín-Vide, J. (2019b) Combining circulation weather types and daily precipitation modelling to derive climatic precipitation regions in the Pyrenees. *Atmospheric Research*, 220, 181–193. Available from: <https://doi.org/10.1016/J.ATMOSRES.2019.01.018>
- Lemus-Canovas, M., Ninyerola, M., Lopez-Bustins, J.A., Manguan, S. & García-Sellés, C. (2018) A mixed application of an objective synoptic classification and spatial regression models for deriving winter precipitation regimes in the eastern Pyrenees. *International Journal of Climatology*, 39, 2244–2259. Available from: <https://doi.org/10.1002/joc.5948>
- Liebezeit, J.R., Gurney, K.E.B., Budde, M., Zack, S. & Ward, D. (2014) Phenological advancement in arctic bird species: relative importance of snow melt and ecological factors. *Polar Biology*, 37(9), 1309–1320. Available from: <https://doi.org/10.1007/s00300-014-1522-x>
- Lionello, P., Abrantes, F., Gacic, M., Planton, S., Trigo, R. & Ulbrich, U. (2014) The climate of the Mediterranean region: research progress and climate change impacts. *Regional Environmental Change*, 14, 1679–1684. Available from: <https://doi.org/10.1007/s10113-014-0666-0>
- López-Moreno, J.I. (2005) Recent variations of snowpack depth in the central Spanish Pyrenees. Arctic, Antarctic, and alpine research. *Institute of Arctic and Alpine Research*, 37(2), 253–260. Available from: [https://doi.org/10.1657/1523-0430\(2005\)037\[0253:RVOSDI\]2.0.CO;2](https://doi.org/10.1657/1523-0430(2005)037[0253:RVOSDI]2.0.CO;2)
- López-Moreno, J.I., Gascoin, S., Herrero, J., Sproles, E.A., Pons, M., Alonso-González, E. et al. (2017) Different sensitivities of snowpacks to warming in Mediterranean climate mountain areas. *Environmental Research Letters*, 12(7), 074006. Available from: <https://doi.org/10.1088/1748-9326/aa70cb>
- López-Moreno, J.I., Goyette, S., Vicente-Serrano, S.M. & Beniston, M. (2011) Effects of climate change on the intensity and frequency of heavy snowfall events in the Pyrenees. *Climatic Change*, 105, 489–508. Available from: <https://doi.org/10.1007/s10584-010-9889-3>
- López-Moreno, J.I., Soubeyroux, J.M., Gascoin, S., Alonso-González, E., Durán-Gómez, N., Lafaysse, M. et al. (2020) Long-term trends (1958–2017) in snow cover duration and depth in the Pyrenees. *International Journal of Climatology*, 40, 6122–6136. Available from: <https://doi.org/10.1002/joc.6571>
- López-Moreno, J.I. & Vicente-Serrano, S.M. (2007) Atmospheric circulation influence on the interannual variability of snowpack in the Spanish Pyrenees during the second half of the 20th century. *Hydrology Research*, 38(1), 33–44. Available from: <https://doi.org/10.2166/nh.2007.030>
- Lorenzo-Lacruz, J., Vicente-Serrano, S.M., López-Moreno, J.I., Beguería, S., GarcíaRuiz, J.M. & Cuadrat, J.M. (2010) The impact of droughts and water management on various hydrological systems in the headwaters of the Tagus River (Central Spain). *Journal of Hydrology*, 386, 13–26. Available from: <https://doi.org/10.1016/j.jhydrol.2010.01.001>
- Martínez-Artigas, J., Lemus-Canovas, M. & Lopez-Bustins, J.A. (2021) Precipitation in peninsular Spain: influence of teleconnection indices and spatial regionalization. *International Journal of Climatology*, 41, 1320–1335. Available from: <https://doi.org/10.1002/joc.6770>
- Martín-Vide, J. 1986. Notes per a la definició d'un índex de “desordre” en pluviometria. *Treballs de la Societat Catalana de Geografia*, 89–96.
- Martín-Vide, J. (2004) Spatial distribution of a daily precipitation concentration index in peninsular Spain. *Int. J. Climatol.*, 24: 959–971. <https://doi.org/10.1002/joc.1030>
- Martín-Vide, J. & Lopez-Bustins, J.A. (2006) The Western Mediterranean oscillation and rainfall in the Iberian Peninsula. *International Journal of Climatology*, 26(11), 1455–1475. Available from: <https://doi.org/10.1002/joc.1388>
- Martín-Vide, J., Lopez-Bustins, J.A., Lemus-Cánovas, M., Moreno-García, M.C., Balagué, X., Gonzalez-Hidalgo, J.C. et al. (2022) The consecutive disparity of precipitation in conterminous Spain. *Theoretical and Applied Climatology*, 147(3–4), 1151–1161. Available from: <https://doi.org/10.1007/s00704-021-03877-6>
- Martín-Vide, J. & Olcina, J. (2001) *Climas y tiempos de España. Spanish, climates and weathers in Spain*. Alianza Editorial: Madrid.
- Morán-Tejeda, E., Lorenzo-Lacruz, J., López-Moreno, J.I., Rahman, K. & Beniston, M. (2014) Streamflow timing of mountain rivers in Spain: recent changes and future projections. *Journal of Hydrology*, 517, 1114–1127. Available from: <https://doi.org/10.1016/j.jhydrol.2014.06.053>

- Navarro-Serrano, F. & López-Moreno, J.I. (2017) Análisis espacio-temporal de los eventos de nevadas en el pirineo Español y su relación con la circulación atmosférica. *Cuadernos de Investigación Geográfica*, 43(1), 233–254. Available from: <https://doi.org/10.18172/cig.3042>
- Notarnicola, C. (2022) Overall negative trends for snow cover extent and duration in global mountain regions over 1982–2020. *Scientific Reports*, 12, 13731. Available from: <https://doi.org/10.1038/s41598-022-16743-w>
- O’Gorman, P.A. (2014) Contrasting responses of mean and extreme snowfall to climate change. *Nature*, 512, 416–418. Available from: <https://doi.org/10.1038/nature13625>
- Pereira, P., Oliva, M. & Misiune, I. (2016) Spatial interpolation of precipitation indexes in Sierra Nevada (Spain): comparing the performance of some interpolation methods. *Theoretical and Applied Climatology*, 126, 683–698. Available from: <https://doi.org/10.1007/s00704-015-1606-8>
- Pérez-Palazón, M.J., Pimentel, R. & Polo, M.J. (2018) Climate trends impact on the snowfall regime in Mediterranean Mountain areas: future scenario assessment in Sierra Nevada (Spain). *Water*, 10(6), 720. Available from: <https://doi.org/10.3390/W10060720>
- Revuelto, J., Gómez, D., Alonso-González, E., Vidaller, I., Rojas-Heredia, F., Deschamps-Berger, C. et al. (2022) Intermediate snowpack melt-out dates guarantee the highest seasonal grasslands greening in the Pyrenees. *Scientific Reports*, 12(1), 1–11. Available from: <https://doi.org/10.1038/s41598-022-22391-x>
- Riehl, H. (1949) Some aspects of Hawaiian rainfall. *The Bulletin of the American Meteorological Society*, 30, 176–187. Available from: <https://doi.org/10.1175/1520-0477-30.5.176>
- Rodríguez-Puebla, C., Encinas, A.H., Nieto, S. & Garmendia, J. (1998) Spatial and temporal patterns of annual precipitation variability over the Iberian Peninsula. *International Journal of Climatology*, 18, 299–316.
- Saffioti, C., Fischer, E.M., Scherrer, S.C. & Knutti, R. (2016) Reconciling observed and modelled temperature and precipitation trends over Europe by adjusting for circulation variability. *Geophysical Research Letters*, 43, 8189–8198.
- Segura, J.H., Nilsson, M.B., Schleucher, J., Haei, M., Sparman, T., Székely, A. et al. (2019) Microbial utilization of simple carbon substrates in boreal peat soils at low temperatures. *Soil Biology and Biochemistry*, 135, 438–448. Available from: <https://doi.org/10.1016/j.soilbio.2019.06.006>
- Sospedra-Alfonso, R. & Merryfield, W. (2017) Influences of temperature and precipitation on historical and future snowpack variability over the northern hemisphere in the second generation Canadian earth system model. *Journal of Climate*, 30, 4633–4656. Available from: <https://doi.org/10.1175/JCLI-D-16-0612.1>
- Trigo, R., Xoplaki, E., Zorita, E., Luterbacher, J., Krichak, S., Alpert, P. et al. (2006) Chapter 3 relations between variability in the Mediterranean region and mid-latitude variability. *Developments in Earth and Environmental Sciences*, 4, 176–226. Available from: [https://doi.org/10.1016/S1571-9197\(06\)80006-6](https://doi.org/10.1016/S1571-9197(06)80006-6)
- Trigo, R.M., Pozo-Vázquez, D., Osborn, T.J., Castro-Diez, Y., Gámiz-Fortis, S. & Esteban-Parra, M.J. (2004) North Atlantic oscillation influence on precipitation, river flow and water resources in the Iberian Peninsula. *International Journal of Climatology*, 24(8), 925–944. Available from: <https://doi.org/10.1002/joc.1048>
- Vicente-Serrano, S.M. & Trigo, R.M. (2011) Hydrological, socioeconomic and ecological impacts of the North Atlantic oscillation in the Mediterranean region. In: *Advances in Global Change Research Series*, Vol. 46. Dordrecht, The Netherlands: Springer, p. 236.
- Wallace, J.M. & Gutzler, D.S. (1981) Teleconnections in the geopotential height field during the northern hemisphere winter. *Monthly Weather Review*, 109, 784–812. Available from: [https://doi.org/10.1175/1520-0493\(1981\)109<0784:TITGHF.2.0.CO;2](https://doi.org/10.1175/1520-0493(1981)109<0784:TITGHF.2.0.CO;2)
- Wang, C., Yang, K. & Zhang, F. (2020) Impacts of soil freeze–thaw process and snow melting over Tibetan plateau on Asian summer monsoon system: a review and perspective. *Frontiers in Earth Science*, 8, 133. Available from: <https://doi.org/10.3389/feart.2020.00133>
- Wipf, S. & Rixen, C. (2010) A review of snow manipulation experiments in Arctic and alpine tundra ecosystems. *Polar Research*, 29, 95–109. Available from: <https://doi.org/10.1111/j.1751-8369.2010.00153.x>

How to cite this article: Lemus-Canovas, M., Alonso-González, E., Bonsoms, J., & López-Moreno, J. I. (2024). Daily concentration of snowfalls in the mountains of the Iberian Peninsula. *International Journal of Climatology*, 44(2), 485–500. <https://doi.org/10.1002/joc.8338>